ISSN 1070-3632, Russian Journal of General Chemistry, 2007, Vol. 77, No. 7, pp. 1275–1283. © Pleiades Publishing, Ltd., 2007.
Original Russian Text © S.V. Zaitseva, S.A. Zdanovich, O.I. Koifman, 2007, published in Zhurnal Obshchei Khimii, 2007, Vol. 77, No. 7, pp. 1194–1202.

Effect of Pyridine on the Reaction of "Spanned" Zinc Porphyrin with Organic Peroxides

S. V. Zaitseva, S. A. Zdanovich, and O. I. Koifman

Institute of Solution Chemistry, Russian Academy of Sciences,
ul. Akademicheskaya 1, Ivanovo, 153045 Russia
e-mail: svz@isc-ras.ru

Received November 23, 2006

Abstract—The reaction of "spanned" zinc porphyrin with organic peroxides in the presence of pyridine at 298 K was studied. The kinetic characteristics of the reaction were obtained. The presence of pyridine favors the formation of the zinc chlorin complex. The nature of the nitrogen base affects the character and rate of the reactions of the zinc porphyrin with peroxide. The structures of the sterically strained metal porphyrin and of the chlorin complex formed in the reaction were optimized by PM3 calculations. As follows from the geometric structure of the macrocyclic compounds, the deformations of the macroring enhance in going from zinc porphyrin to zinc chlorin.

DOI: 10.1134/S1070363207070213

The interest in macrocyclic compounds is primarily caused by the diversity of their useful properties and possibility of using them for simulating natural biocoordination systems [1–4]. An analog of one of such processes in natural systems is the reaction of metal porphyrins and phthalocyanines with peroxides under aerobic conditions.

Previously we studied the oxidative degradation of "spanned" zinc porphyrin with the 2,5-dimethoxyphenylene "lid," effected by *o*-xylene peroxides, both in the presence of a nitrogen-containing base and without it [5, 6]. Introduction of imidazole into the system made the reaction several times faster. Variation of the imidazole concentration appeared to be an efficient factor determining the kinetics of the decomposition of the zinc complex.

In this study, with the aim of further systematic investigation of the behavior of sterically strained zinc porphyrins in reactions with compounds containing available oxygen, we examined how the nature of the nitrogen-containing base affects the character and rate of the reaction of the macrocyclic complex with organic peroxides.

Reagent-grade xylenes and toluene contained sufficient amounts of organic peroxides capable of redox reactions with metal porphyrins (MPs) [7–10]. Both the central metal atom and the macroring can undergo oxidation [7–13].

In the previously studied processes [5, 6], the macroring is oxidized first. Two principally different mechanisms of the oxidation of a spanned zinc porphyrin with organic peroxides are possible: (1) hydroxylation [12] and (2) free-radical reaction [14].

The first reaction is characterized by the transition of two π electrons from the macroring to the σ levels and by binding with the RO and OH groups of the peroxide [reaction (I)]. Such transformations are accompanied by distortion of the conjugation of the tetrapyrrole fragment and increase in its deformation. As a result, an unstable product is formed, which undergoes further transformations with the macroring cleavage.

Reaction (I) is the limiting step. Further degradation of the chromophore is fast, because the intermediate product was not detected in the absorption spectra (Fig. 1a).

In the second case, the radicals $RO^{\cdot}$ and $HO^{\cdot}$ generated by activation of the peroxide react with a sterically strained sinc porphyrin at the meso position with the formation of new radicals.

The metal porphyrin radical formed by reactions (III)–(VIII) is in the excited state and is very unstable. Therefore, in the course of the reaction it undergoes further transformations leading to decolorization of the solution. The formation of the macrocyclic radical is probably the limiting step in this case. All the subsequent steps should be faster.

The presence of imidazole does not alter the character of the oxidation of zinc porphyrin. Variation of the concentration of the nitrogen-containing base affects only the reaction rate [6].

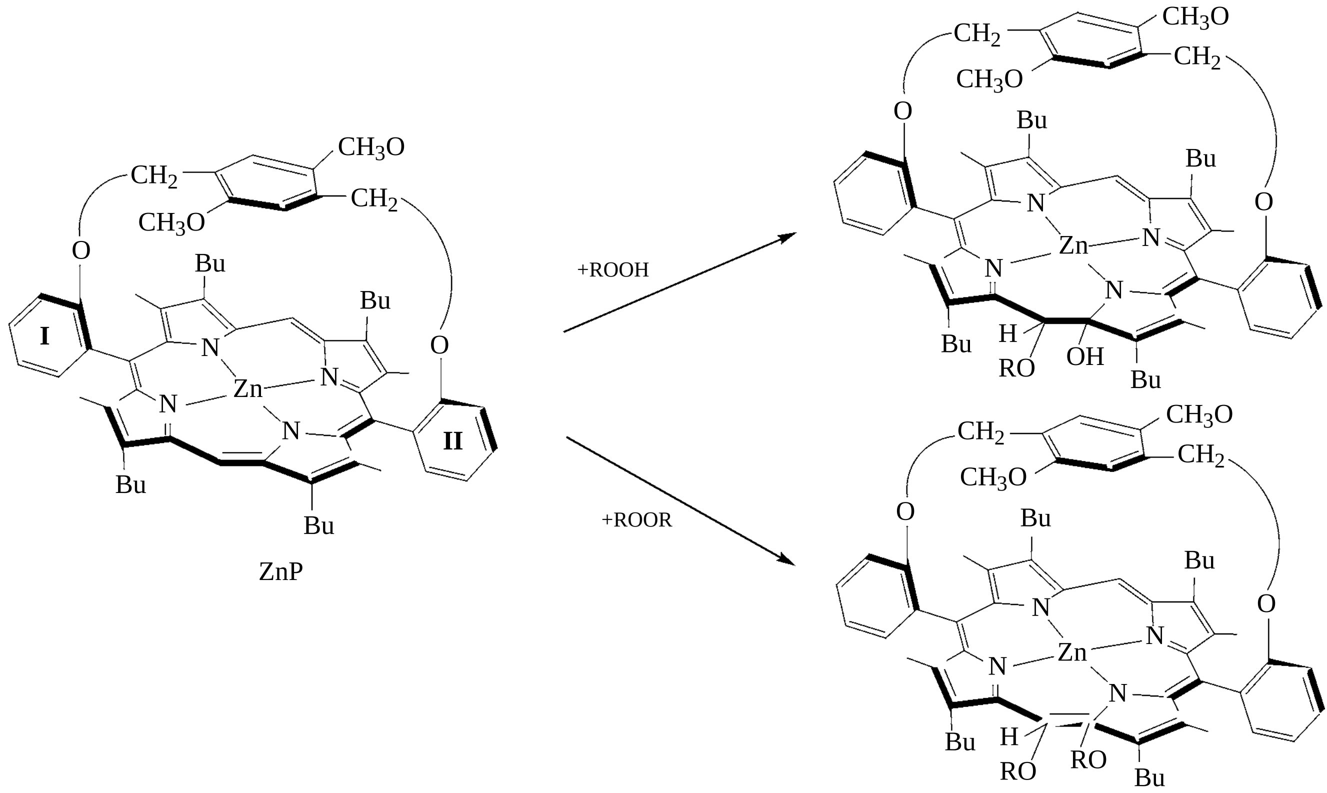

(I)

$$\mathrm{ROOR} \longrightarrow 2\mathrm{RO}^{\bullet},$$
$$\mathrm{ROOH} \longrightarrow \mathrm{RO}^{\bullet} + \mathrm{HO}^{\bullet}, \qquad \text{(II)}$$

$$\mathrm{ZnP} + \mathrm{RO{-}|{-}OR} = \mathrm{ZnP}^{\bullet}(\mathrm{RO}) + \mathrm{RO}^{\bullet}, \qquad \text{(III)}$$

$$\mathrm{ZnP} + \mathrm{RO{-}|{-}OH} = \mathrm{ZnP}^{\bullet}(\mathrm{RO}) + \mathrm{HO}^{\bullet}, \qquad \text{(IV)}$$

$$\mathrm{ZnP} + \mathrm{RO{-}|{-}OH} = \mathrm{ZnP}^{\bullet}(\mathrm{HO}) + \mathrm{RO}^{\bullet}, \qquad \text{(V)}$$

$$\mathrm{ZnP} + \mathrm{RO{-}|{-}OR} = \mathrm{ZnP}^{\bullet} + \mathrm{ROH} + \mathrm{RO}^{\bullet}, \qquad \text{(VI)}$$

$$\mathrm{ZnP} + \mathrm{RO{-}|{-}OH} = \mathrm{ZnP}^{\bullet} + \mathrm{ROH} + \mathrm{HO}^{\bullet}, \qquad \text{(VII)}$$

$$\mathrm{ZnP} + \mathrm{RO{-}|{-}OH} = \mathrm{ZnP}^{\bullet} + \mathrm{RO}^{\bullet} + \mathrm{H_2O}. \qquad \text{(VIII)}$$

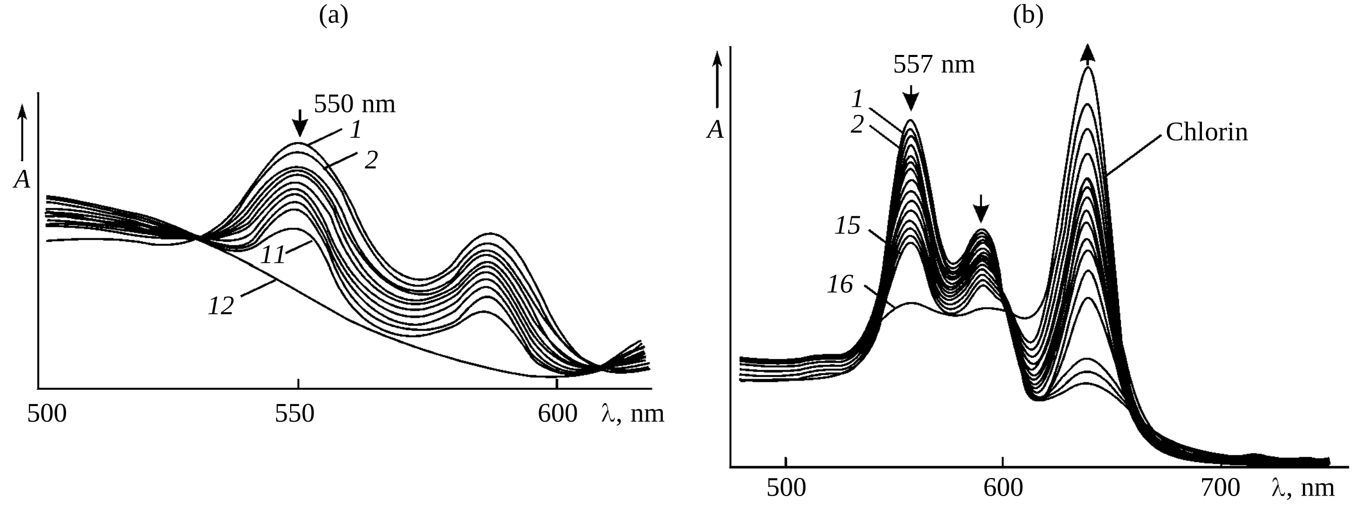

Fig. 1. Electornic absorption spectra: (a) ZnP in *o*-xylene (c_{ZnP} 1.54×10^{-5} M, c_{perox} 0.9×10^{-6} M) at 298 K; τ, s: (*1*) 0, (*12*) 38600, and (*2*–*11*) intermediate instants of time; (b) (Py)ZnP (c_{ZnP} 6.44×10^{-6} M, c_{Py} 0.31 M) in *o*-xylene (c_{perox} 1.24×10^{-5} M) at 298 K; τ, s: (*1*) 0, (*16*) 49200, and (*2*–*15*) intermediate instants of time.

Addition of pyridine (*c* 3.10×10^{-1} M) to the system ZnP (*c* 6.44×10^{-6} M)–peroxide (*c* 1.24×10^{-5}–3.09×10^{-5} M) at 298 K leads to the formation of a chlorin complex (Fig. 1b). The pyridine concentration in the system is sufficiently high ($c_{Py} >> c_{ZnP}$) for virtually instantaneous formation of the extra complex (Py)ZnP, and the macrocyclic compound is reduced to zinc chlorin in the form of the extra complex only. In this case, stepwise reaction (IX) occurs:

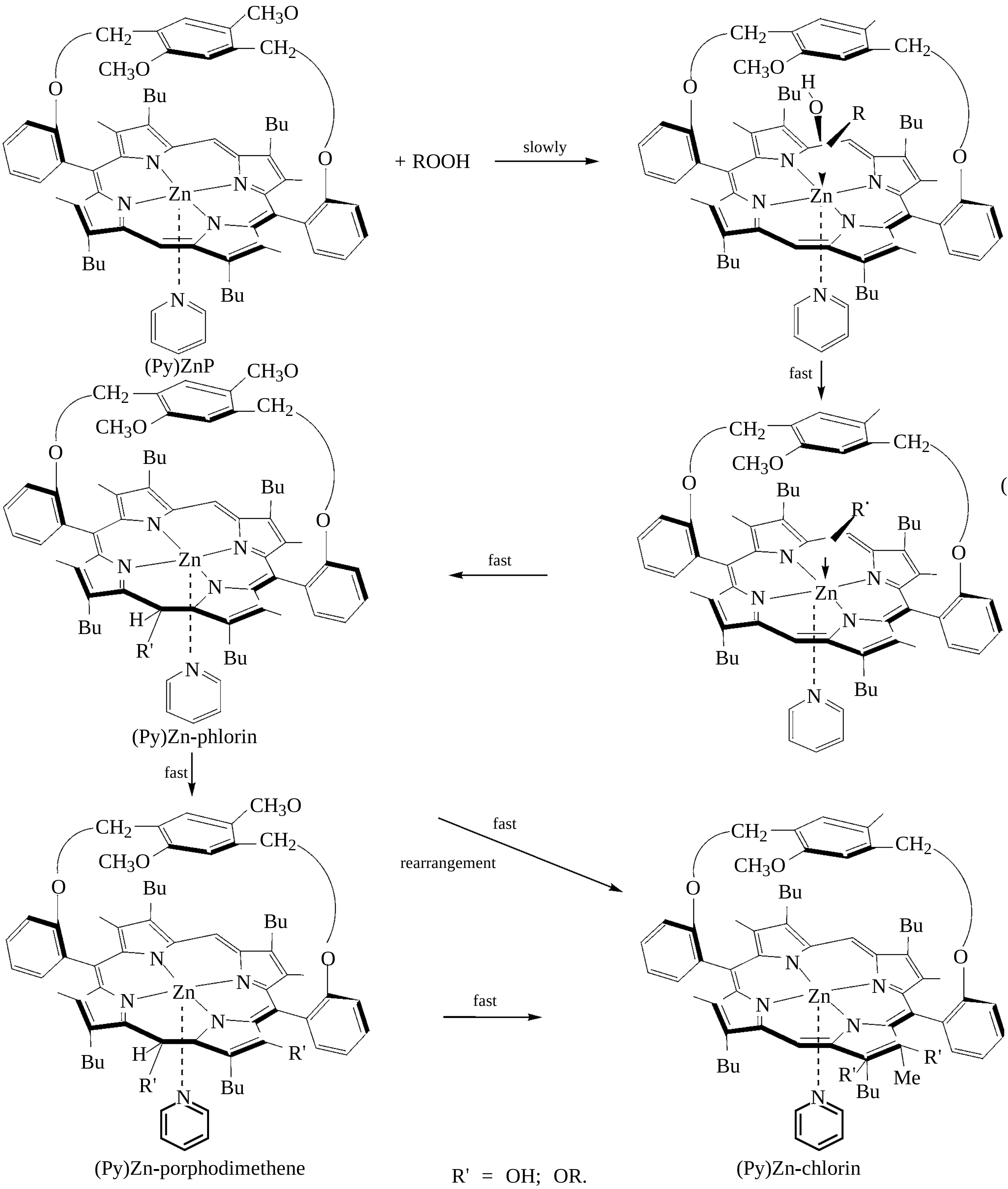

(IX)

R' = OH; OR.

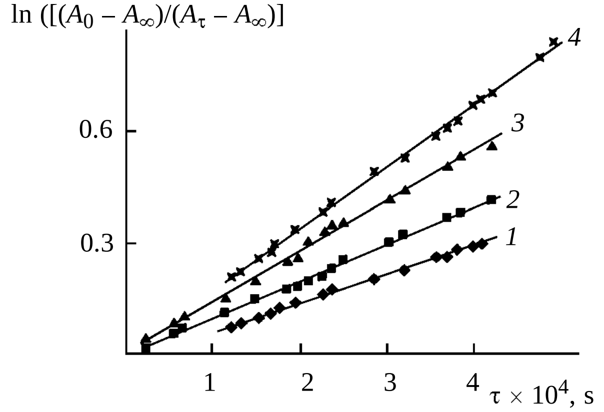

Fig. 2. Plot of $\ln[(A_0 - A_\infty)/(A_\tau - A_\infty)]$ vs. τ for the reaction of (Py)ZnP with peroxides. c_{perox}, M: (*1*) 1.24×10^{-5}, (*2*) 1.86×10^{-5}, (*3*) 2.48×10^{-5}, and (*4*) 3.09×10^{-5}; c_{ZnP} 6.44×10^{-6} M; c_{Py} 3.1×10^{-1} M.

The reduction of the metal porphyrin in the presence of pyridine to the chlorin complex is accompanied by the oxidation of organic peroxides. The low concentrations of the reactants (10^{-5}–10^{-6} M) do not allow visual observation of the oxygen evolution in the course of oxidation.

The order of the reduction with respect to the (Py)ZnP concentration is close to unity, as seen from the satisfactory constancy of k_{app} (Table 1) of formally first order (n 1):

$$dc_{(\text{Py})\text{ZnP}}/d\tau = kc^{n}_{(\text{Py})\text{ZnP}}. \qquad (1)$$

The apparent rate constants k_{app} given in Table 1 were obtained both from the equation $k_{\text{app}} = (1/\tau) \times \ln[(A_0 - A_\infty)/(A_\tau - A_\infty)]$ and by processing of the linear relationship $\ln[(A_0 - A_\infty)/(A_\tau - A_\infty)]$–τ (Fig. 2). The values of k_{app} obtained by calculation and graphically agree within 1–2%. The constants k_{app} linearly increase with the peroxide concentration (Fig. 3). The constants relate to the slow step of the reaction of the peroxide and the complex.

By least-squares treatment of the linear relationship $\log k_{\text{app}} = \log k_{\text{c}} + m \log[\text{peroxide}]$, we determined the true constant (k_v 0.525 $\text{s}^{-1}\,\text{mol}^{-1}\,\text{l}$) and the reaction order with respect to the peroxide (m 1) (Fig. 3).

Table 1. Kinetic parameters of the reduction of ZnP with *o*-xylene peroxides at T 298 K in the presence of pyridine (c_{ZnP} 6.44×10^{-6} M, c_{Py} 0.31 M)

$c_{\text{perox}} \times 10^5$, M	$k_{\text{app}} \times 10^5$, s^{-1}
1.24	0.724 ± 0.038
1.86	0.949 ± 0.058
2.48	1.39 ± 0.070
3.09	1.77 ± 0.170

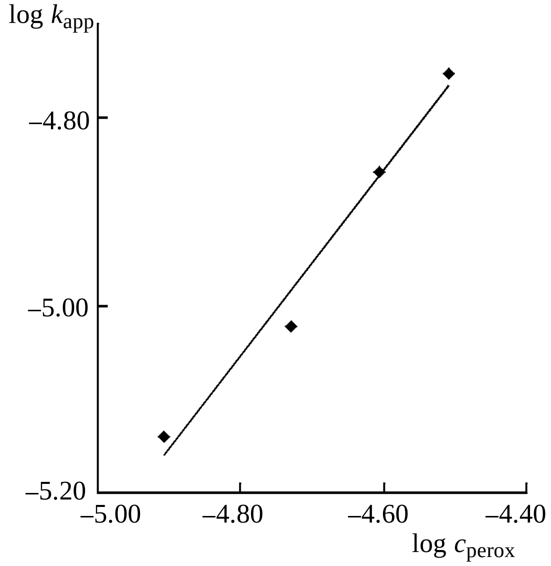

Fig. 3. Plot of $\log k_{\text{app}}$ vs. $\log c_{\text{perox}}$ at $c_{\text{perox}} > c_{(\text{Py})\text{ZnP}}$. $\log k_{\text{app}} = 0.9947 \log c_{\text{perox}} - 0.2797$, $r = 0.9773$.

The rate equation for the reaction of (Py)ZnP with peroxide is as follows:

$$-dc_{\text{perox}} = k_v[(\text{Py})\text{ZnP}][\text{peroxide}]. \qquad (2)$$

The effect of pyridine on the character of the reaction of the zinc porphyrin with peroxides, differing from that exerted by imidazole (Im), is associated with the possibility of the coordination of a peroxide molecule by the zinc atom. The Zn–Py bond strength is insufficient because of the lower basicity of Py compared to Im [15]. Therefore, an effective positive charge sufficient for the interaction with a peroxide molecule remains on the Zn atom. The formation of a weak Zn–ROOH bond is accompanied by activation of the peroxide molecule, and the RO┼OH bond is broken with the generation of the $\text{RO}^{\cdot}$ and $\text{HO}^{\cdot}$ radicals. One of them remains bound to the zinc atom. In this case, the electron density from the radical is transferred to the metal atom and redistributed over the whole macroring, which ultimately leads to its reduction [reaction (IX)]. The free radicals generated in the course of the reduction decay by recombination.

It should be noted that the deformation of the (L)ZnP macroring affects the course of the process. The structural features of the molecular complex and the steric strains in it were evaluated by quantum-chemical calculation of the molecules of zinc porphyrin, its extra complex, and zinc chlorin, with optimization of the geometry (Table 2). We found that ZnP has a nonplanar structure with tertiary nitrogen atoms projecting into the bulk of the solvent (Fig. 4). The

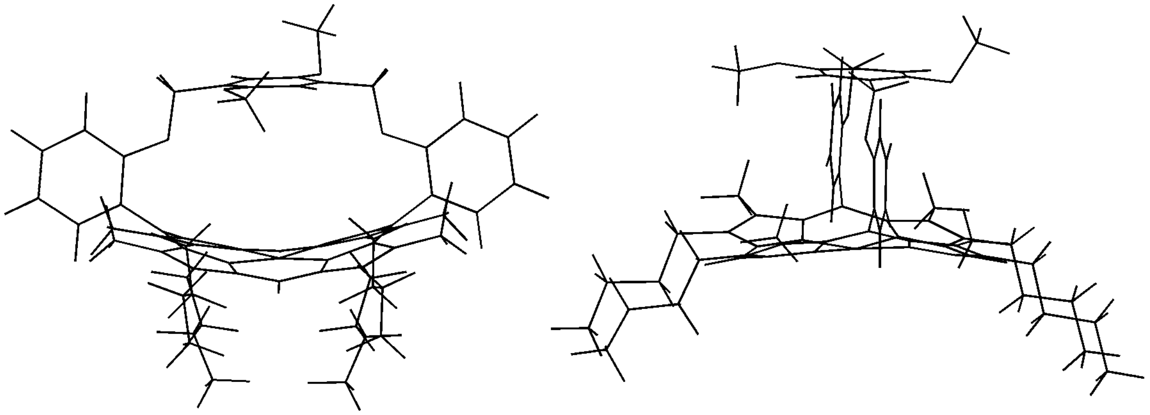

ZnP

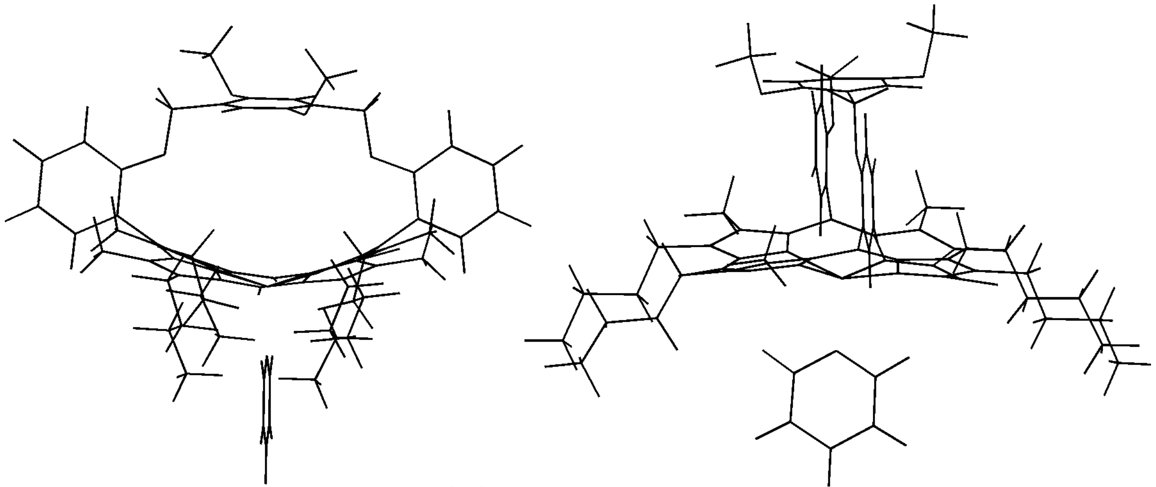

(Py)ZnP

Fig. 4. Molecular structure of zinc porphyrin and its extra complex, according to PM3 calculations.

Table 2. Some geometric characteristics of “spanned” zinc porphyrin, its extra complex, and zinc chlorin[a]

Complex	N^{21}–N^{23}, N^{22}–N^{24}, Å	Zn–N_L, Å	Ct–Zn, Å	Zn–N^{21}, Zn–N^{23}, Å	Zn–N^{22}, Zn–N^{24}, Å	C^{17}–O, Å	C^{18}–O, Å	C_{1phI}–C_{1phII},[b] Å	$N^{21}ZnN^{23}$, deg	$N^{22}ZnN^{24}$, deg
ZnP	4.0485 4.0668		0.1349	2.0492 2.0083	2.0505 2.0278			9.1478	173.38	171.37
(Im)ZnP	4.0864 4.0858	2.0763	0.4601	2.1031 2.0856	2.1050 2.0835			9.1154	154.62	154.56
(Py)ZnP	4.0965 4.0864	2.0984	0.4518	2.0840 2.1110	2.0807 2.1080			9.1359	155.12	154.59
(Py)ZnCh$(OH)_2$	4.0738 4.1031	2.0946	0.4965	2.0918 2.1013	2.1014 2.1077	1.4177	1.4222	9.1147	152.60	154.23
(Py)ZnCh$(R)_2$	4.0712 4.1371	2.1016	0.4780	2.0918 2.0901	2.1074 2.1322	1.4274	1.4319	9.1216	153.57	154.75
(Py)ZnCh(OH)(R)	4.0696 4.1207	2.0989	0.4746	2.0915 2.0874	2.1003 2.1184	1.4128	1.4367	9.1023	153.74	155.24
(Py)ZnCh(R)(OH)	4.0641 4.1321	2.0959	0.4998	2.0919 2.0933	2.1062 2.1196	1.4281	1.4138	9.1329	152.36	155.82

[a] The atom numbering is in accordance with the literature [16]. [b] Distance between two carbon atoms of phenyl fragments (I) and (II).

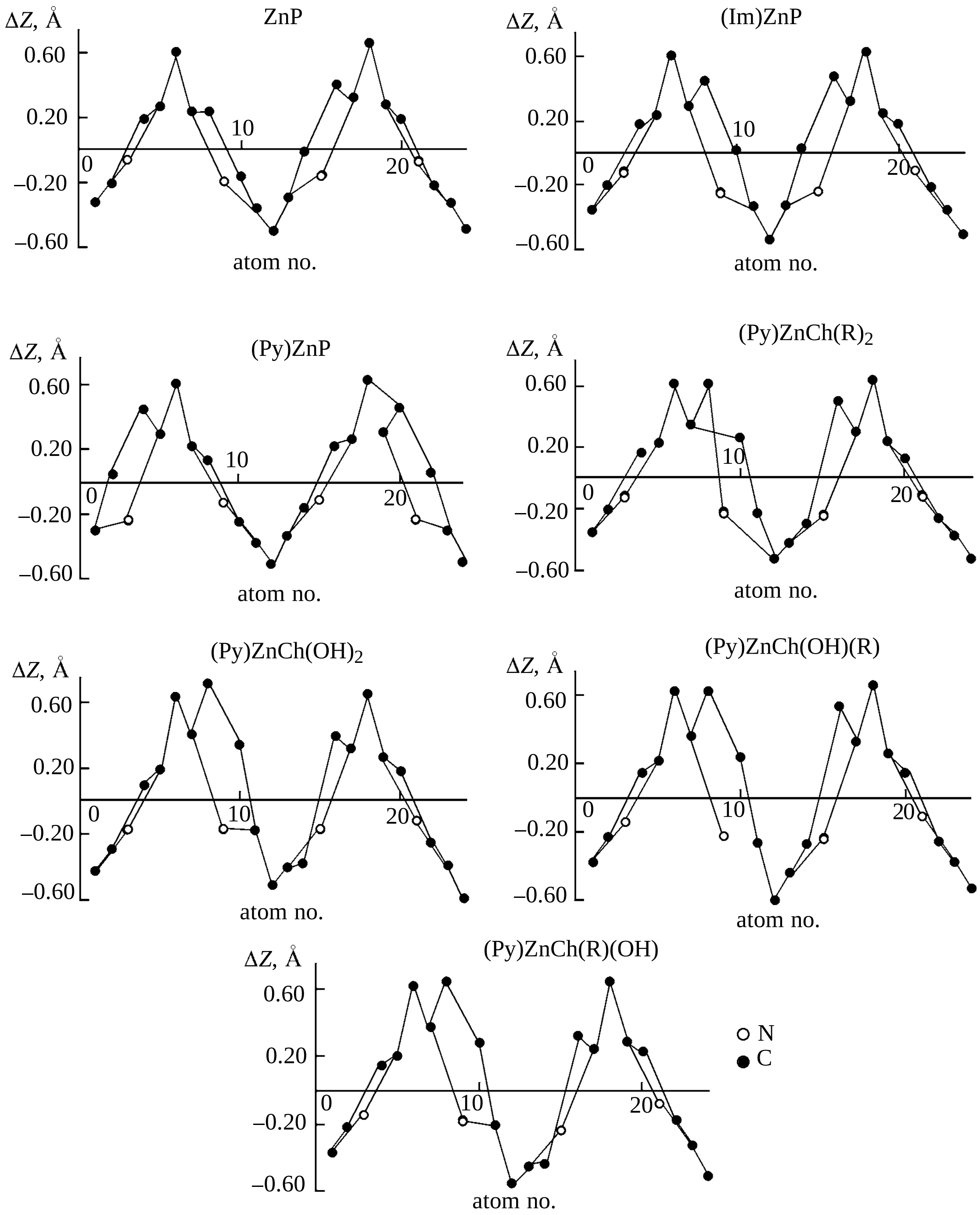

Fig. 5. Deviations from the mean molecular plane (Δ*Z*) of core atoms of the porphyrin macroring in the "spanned" zinc porphyrin, its molecular complexes with nitrogen-containing bases, and complexes of zinc chlorins with pyridine, according to PM3 calculations.

phenyl substituents together with methylene links of the porphyrin fragment are inclined toward the "lid" (deviation from the mean N_4 plane 26.5°), and the other two methylene links that do not bear functional groups are inclined to the opposite side. As a result, the macroring becomes saddle-shaped. The C^{m20}–Zn–C^{m10} and C^{m5}–Zn–C^{m15} angles are 150.1° and 172.1°, respectively. The "lid" is arranged virtually parallel to the N_4 plane, with a small (2°–3°) deviation. Methoxy groups are oriented differently: one of them is in the phenyl "lid" plane, and the other projects from the plane at an angle of 113.5°. The atoms deviate from the mean molecular plane (Fig. 5). As seen from the diagram in Fig. 5, the two pyrrole fragments of the complex are subject to a small twisting deformation. The geometric characteristics show that the molecule of the complex is strained and deformed (Table 2; Figs. 4, 5).

Interaction of the zinc atom with pyridine gives rise to the cis effect in the extra complex. The electronic and steric structures of the zinc porphyrin change (Table 2, Fig. 4). The effective charge on the Zn atom decreases by 0.154 *e*. The angle of inclination of the phenyl substituents increases by 4°. The C^{m20}–Zn–C^{m10} and C^{m5}–Zn–C^{m15} angles are 139.5° and 175.7°, respectively. Both methoxyl substituents of the "lid" project from the phenylene plane by 114°. The internal angles N^n–Zn–N^{n+1} of the N_4 cavity decrease by 2°–3°. The pyridine coordination is also accompanied by an increase in the deviation of the Zn atom from the macroring planbe, increase in the size of the N_4 cavity, and weakening of the Zn–N^p bond (Table 2). The deviations of the macroring atoms from the mean molecular plane change. The extent of the twisting deformation of the two adjacent pyrrole fragments increases (Fig. 5). This, in turn, can be accompanied by weakening of the conjugation in them. Analysis of the optimized molecular structures shows that the covalent C^p–R' bond is formed just in these pyrrole fragments in the β position.

It should be noted that, upon coordination of imidazole, the ZnP molecule becomes somewhat more strained (Fig. 5, Table 2). In particular, the phenyl substituents are oriented at an angle of 33° relative to the N_4 plane. The C^{m20}–Zn–C^{m10} and C^{m5}–Zn–C^{m15} angles are 137.5° and 176.2°, respectively. The deviation of the Zn atom from the N_4 plane (Zn–Ct) and the strength of the Zn–N_L bond somewhat exceed the respective characteristics of the complex (Py)ZnP (Table 2). An increase in the deformation is accompanied by a decrease in the aromaticity of the macroring, which, in turn, leads to an increase in its basicity. The presence of the Zn–Im bond in the complex leads to a change in the charge on the metal atom. According to a quantum-chemical calculation, the charge on the Zn atom is lower by 0.4 e than that in the (Py)ZnP molecule. Therefore, as already noted, formation of a peroxide–zinc bond in the complex (Im)ZnP is improbable.

The formation of (Py)Zn-chlorin is accompanied by further enhancement of the macroring strain (Table 2; Figs. 5, 6). Three types of structures of chlorin molecules, one of them having an isomer, can exist. All of them have a nonplanar saddle-like structure (Fig. 6). In the complexes (Py)ZnCh, the angle of inclination of the phenyl fragments increases by 1°–4.5°, and the cavity between them contracts by 0.0143–0.0336 Å. The exception is (Py)ZnCh(R)(OH) in which this angle and the cavity size do not change. The angles C^{m20}–Zn–C^{m10} and C^{m5}–Zn–C^{m15} change by 1°–3°. The asymmetry of the N_4 plane becomes more pronounced (Table 2). The formation of the C^p–R' bond leads also to a considerable increase in the twisting deformation of the pyrrole fragments [four in the case of $(Py)ZnCh(R)_2$ and three in the other cases] (Fig. 5). The angles in these pyrroles also change. For example, in $(Py)ZnCh(R)_2$, in the pyrrole fragment bearing the R' substituents, the angles are 110.01°, 103.39°, 100.39°, and 112.41°, whereas in (Py)ZnP they are 108.39°, 107.77°, 107.20°, and 108.95°. The Zn–Ct distance increases by 0.0228–0.0480 Å, whereas the Zn–N_L distance varies irregularly (Table 2).

Thus, our results show that the nature of the base incorporated in the porphyrin complex and the degree of strain of the macroring significantly affect the course of the redox reaction involving available oxygen.

EXPERIMENTAL

"Spanned" porphyrin [17]. A solution of 0.28 g of chloroacetic acid in 30 ml of acetonitrile was added with stirring in a nitrogen atmosphere to a solution of 0.66 g of 3,3'-dibutyl-4,4'-dimethyldipyrromethane and 0.51 g of 2,5-bis(2'-formylphenoxymethyl)-1,4-dimethoxybenzene in 200 ml of acetonitrile. The mixture was stirred in the dark for 4 h, after which 0.85 g of o-chloranil in 10 ml of THF was added, and the mixture was allowed to stand for 12 h at room temperature. The solvent was distilled off, and the residue was washed with an alkali solution and water and then dried. After dissolution in chloroform and double chromatography on alumina in chloroform, the porphyrin was precipitated with methanol and dried. Yield 0.42 g (39.4%). R_f (Silufol): 0.44 (chloroform). Electronic absorption spectrum, λ_{max}, nm (log ε): 639 (3.57), 585 (3.84), 551 (3.83), 516 (4.18), 419 (5.32) ($CHCl_3$). ^1H NMR spectrum, δ, ppm: 9.743 (ms-H), 8.929 d, 7.615 d, 7.048 d (Ph), 3.857 m, 2.145 m, 1.744 m, 1.151 t (Bu), 3.476 s (OCH_2), 3.434 s (R–H), 2.705 s, 2.548 s (Me), 1.852 s (OCH_3), –2.553 s (NH).

Zin complex of "spanned" porphyrin (ZnP) [18] was prepared by heating the porphyrin in benzene with a tenfold excess of zinc acetate for 2 h. Then excess salt was washed out with water. The solution was concentrated by vacuum evaporation to a volume of 5–10 ml and chromatographed two times on alumina (Brockmann grade II, eluent benzene). The zinc complex was precipitated with methanol and dried. Yield 95%. Electronic absorption spectrum (*o*-xylene),

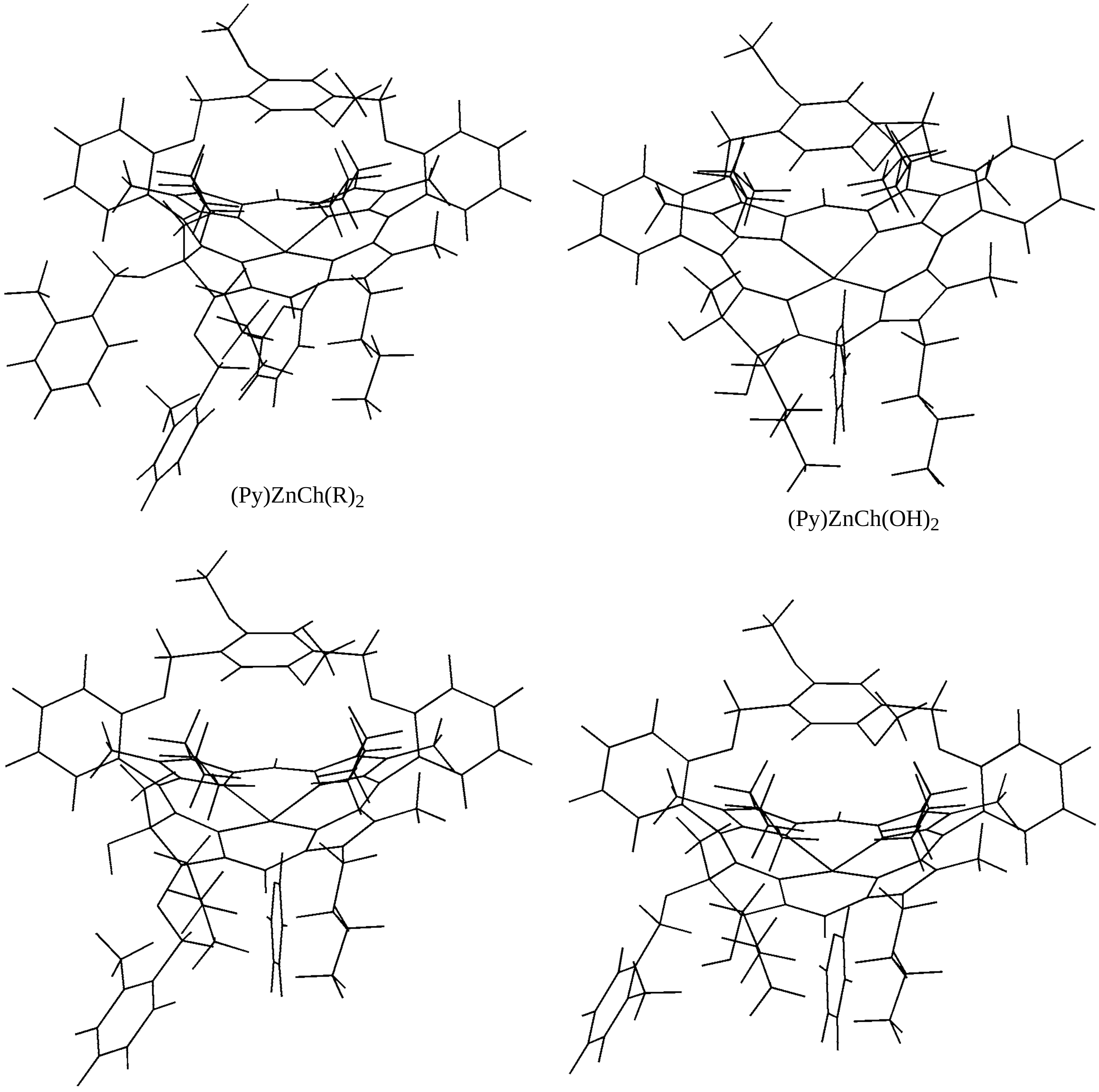

(Py)ZnCh(R)$_2$

(Py)ZnCh(OH)$_2$

(Py)ZnCh(OH)(R)

(Py)ZnCh(R)(OH)

Fig. 6. Molecular structure of zinc chlorin derivatives, according to PM3 calculations.

λ_{max}, nm (log ε): 587.0 (4.22), 549.0 (4.43), 410.0 (5.34). Found, %: C 74.58, H 7.23, N 5.56. $C_{62}H_{70}\cdot ZnN_4O_4$. Calculated, %: C 74.42, H 7.05, N 5.60.

The reaction kinetics was monitored spectrophotometrically [19] (working wavelength 555 nm) at 298 K in *o*-xylene. The rate constants of the reaction of (Py)ZnP with a peroxy compound in *o*-xylene were calculated by a formally first-order rate equation, provided that the peroxide is in excess relative to the metal porphyrin:

$$k_{app} = \frac{1}{\tau} \ln \frac{A_0 - A_\infty}{A_\tau - A_\infty}, \tag{3}$$

where A_0, A_τ, and A_∞ are the initial, running, and final optical densities at the working wavelength for the metal porphyrin, respectively.

Optimization of k_{app} and determination of the rms deviations were performed by the least-squares method using the Microsoft Excel programs; consistent results were obtained. The relative error in the determination of k_{app} was 5–10%.

The electronic absorption spectra were recorded on AF-26 and Specord M-400 devices. The ^{1}H NMR spectra were taken on a Bruker AC-200 spectrometer (200 MHz, internal reference HMDS) in $CDCl_3$.

Quantum-chemical calculations were performed by the PM3 method in the CNDO approximation [20–23] with full geometry optimization. The optimization was performed to a gradient of 0.06 kJ Å^{-1} mol^{-1}.

ACKNOWLEDGMENTS

The study was supported by the Program for Basic Research of the Russian Academy of Sciences “Theoretical and Experimental Study of the Nature of Chemical Bond and Mechanisms of the Most Important Reactions and Processes” for the year 2006 and by the Russian Foundation for Basic Research (project no. 06-03-325 337-a).

REFERENCES

1. Konovalova, N.V. and Evstigneeva, R.P., *Usp. Khim.*, 2001, vol. 70, no. 11, p. 1059.
2. Evstigneeva, R.P., *Uspekhi khimii porfirinov* (Advances in Porphyrin Chemistry), Golubchikov, O.A., Ed., St. Petersburg: Nauchno-Issled. Inst. Khimii S.-Peterb. Gos. Univ., 1999, vol. 2, p. 115.
3. Sanders, J.K.M., Bampos, N., Clude-Watson, Z., Darling, S.L., Hawley, J.C., Kim, H.-J., Mak, C.C., and Webb, S.J., *The Porphyrin Handbook*, vol. 3, Kadish, K.M., Smith, K.M., and Guilard, R., Eds., New York: Academic, 2000, p. 1.
4. Arai, T. and Sato, Y., *Chem. Lett.*, 1990, no. 4, p. 551.
5. Zaitseva, S.V., Zdanovich, S.A., and Koifman, O.I., *Zh. Neorg. Khim.*, 2003, vol. 48, no. 1, p. 137.
6. Zaitseva, S.V., Zdanovich, S.A., and Koifman, O.I., *Zh. Obshch. Khim.*, 2005, vol. 75, no. 5, p. 847.
7. Buchler, J.W., Lay, K.L., Caste, L., and Ullrich, V., *Inorg. Chem.*, 1982, vol. 21, no. 2, p. 842.
8. Juan, L.-Ch. and Bruice, T.C., *J. Am. Chem. Soc.*, 1985, vol. 107, no. 2, p. 512.
9. Kropf, H., Spangenberg, J., Gunst, A., and Hinrichsen, J., *Justus Liebigs. Ann. Chem.*, 1980, no. 12, p. 1923.
10. Dirk, M. and Hambright, P., *J. Chem. Soc., Faraday Trans.*, 1992, vol. 88, no. 14, p. 2013.
11. Liston, D.J. and West, B.O., *Inorg. Chem.*, 1985, vol. 24, no. 10, p. 1568.
12. Berezin, B.D. and Sennikova, G.V., *Kinet. Katal.*, 1968, vol. 9, no. 3, p. 528.
13. Kalish, H., Camp, J.E., Stepien, M., Latos-Grazynski, L., and Balch, A.L., *J. Am. Chem. Soc.*, 2001, vol. 123, no. 47, p. 11 719.
14. Reichardt, Ch., *Solvents and Solvent Effects in Organic Chemistry*, Weinheim: VCH, 1988.
15. *Tablitsy konstant skorostei i ravnovesii gomoliticheskikh organicheskikh reaktsii* (Tables of Rate and Equilibrium Constants of Homolytic Organic Reactions, Moscow: VINITI, 1976, vol. 2.
16. Koifman, O.I. and Ageeva, T.A., *Uspekhi khimii porfirinov* (Advances in Porphyrin Chemistry), Golubchikov, O.A., Ed., St. Petersburg: Nauchno-Issled. Inst. Khimii S.-Peterb. Gos. Univ., 1997, vol. 1, p. 6.
17. Semeikin, A.S., *Doctoral (Chem.) Dissertation*, Ivanovo: Inst. of Chemistry of Nonaqeuous Solutions, 1995.
18. Zaitseva, S.V., Zdanovich, S.A., Ageeva, T.A., Golubchikov, O.A., and Semeikin, A.S., *Koord. Khim.*, 2001, vol. 27, no. 3, p. 168.
19. *Eksperimental’nye metody khimicheskoi kinetiki* (Experimental Methods of Chemical Kinetics), Emanuel’, N.M. and Sergeev, G.B., Eds., Moscow: Vysshaya Shkola, 1980.
20. Bersuker, I.B., *Elektronnoe stroenie i svoistva koordinatsionnykh soedinenii* (Electronic Structure and Properties of Coordination Compounds), Leningrad: Khimiya, 1986.
21. Fletcher, R., *Methods of Optimization*, New York: Wiley, 1980, p. 45.
22. Stewart, J.J.P., *J. Computer-Aided Mol. Des.*, 1990, vol. 4, no. 4, p. 1.
23. Schmidt, M.W. and Baldridge, K.K., *J. Comput. Chem.*, 1993, vol. 14, no. 11, p. 1347.